24th COBEM - 2017

24th ABCM International Congress of Mechanical Engineering
December 3-8, 2017, Curitiba, PR, Brazil

COBEM-2017-0809
FAULT DIAGNOSTIC FOR ROTATING MACHINES USING BAYESIAN NETWORKS

Tyminski, N. C.
Castro, H. F.
Unicamp - R. Mendeleyev, 200 - Cidade Universitária, Campinas - SP, 13083-860
natalia.tyminski@fem.unicamp.br; heliofc@fem.unicamp.br

Abstract. *The maintenance based on the vibration signal is very common and used nowadays. The rotating machines, even when balanced and aligned, shows some level of vibration. This vibration can be very dangerous when reaches higher vibrations, causing a catastrophic accident. For this reason, it´s important the study of fault diagnostic, once that the failures of this machines contribute for the level of vibrations. This paper aims the use of Bayesian Network to do the fault diagnosis, whereas the symptoms generated by the faults that are taken into account. The considered faults are unbalance, misalignment and crack. The results showed are consistent, besides the prior probabilities considered are based on a few simulated results. The method proved to be consistent and efficiently.*

Keywords: *Fault diagnosis, Bayesian Network, Rotor*

1. INTRODUCTION

The study of rotating machines plays an important role in industrial applications. The energy industry relays on the correct functioning of turbo-generator, considering that failures can stop the production line. These machines are subject to some level of vibration, which can occur by the system itself, or by some component of the system. If this vibration is reaching certain level, that it could be harmful for them. The most probable cause for undesired vibrations can be the shaft misalignment, shaft bow, cracks, the unbalance mass and others undesirable failures. In that case, it´s difficult to quantify how much these components act on the vibration system and how is yours signatures on vibration. There are a lot of study about fault diagnose, most of them uses the vibration analyses to identify the most probable failures. It has been saw that for unbalanced mass, the vibration system will be bigger on first harmonic amplitude. Sekhar and Prabhu (1995) analyzed the effect of coupling misalignment, and they reported the vibration on 2X. Al Hussain and Redmond (2002) study the dynamic response when considering the rigid mechanical coupling with parallel misalignment, and they conclude that there´s no vibration on component 2X.

Petel and Darpe (2008) analyzed the vibration response of a cracked rotor in presence of rotor-stator rub. They considered multiple faults in a rotor system and considered the experiment and simulated results to analyze the vibration response. They concluded that excitations due to unbalance and crack are strongly forward whirling in nature frequency. Lal and Tiwari (2012) developed an algorithm to identify multiple faults in a simple rotor-bearing-coupling system based on force response measurements. This algorithm will estimate the dynamics parameters of bearings and coupling, and residual unbalance. Chen and Mo (2004) uses the wavelet transform techniques for fault diagnose of rotating machine.

There are some works on faults diagnose that uses stochastic techniques. Lei Y. et al. (2008) proposed an adaptive neuro-fuzzy inference. Bayesian Networks were used to diagnose chiller faults (Zhao Y.; Xiao F. and Wang S., 2012) and for fault diagnosis based on operation procedures (Liu Z. et al, 2015). Xu (2012) used Bayesian Networks to fault inference, taken into account the machine symptoms as well as machines running conditions. Jun and Kim (2017) proposes a Bayesian Network-based fault analysis method, where they use as case of study a centrifugal compressed utilized in a plant. Some authors used Bayesian Networks combined with other techniques, for instance, the Particle Swarm Optimization used with Bayesian Networks for fault diagnosis on airplane engines (Sahin F. et al, 2007). Atoui and Kobi (2015) investigated the fault detection using Gaussian Network, that is a special case of Bayesian Networks.

The aim of this work is use Bayesian Networks for fault diagnose in rotating system, based on the symptom´s machine. A few numerical simulations were done, where the system was model with Finite Element Method (FEM) and the failures were included on the model. The frequency vibration at 1X, 2X and 3X are evaluated with sensitivity analyses. At this step, the effects of each failure were analyzed. This information was used to build the topology of Bayesian Network. The paper is organized as follows. The section 2 shows the methodology of the work, the theory about Bayesian

Networks is presented on section 3. The mathematical model of system, as it´s failures, were presented on section 4. Section 5 is the sensitivity analyses, results and discussions are on section 6, and section 7 is the conclusion of this paper.

2. METHODOLOGY

The Figure 1 shows the flowchart of experimental procedures. It consists in 5 steps, the first one is the Model simulation, where the vibration system is obtained by numerical simulation. The second step consist on sensitivity analyses, which takes into account all the effects generated by the faults included on model, and their combination. The third step is the prior probabilities, which is the probabilities of faults based on machine running conditions. The next step are the machine symptoms, which we can determined by the vibration signal of the system. In addition, the last step are the faults diagnostic, which are given by the Bayesian Networks.

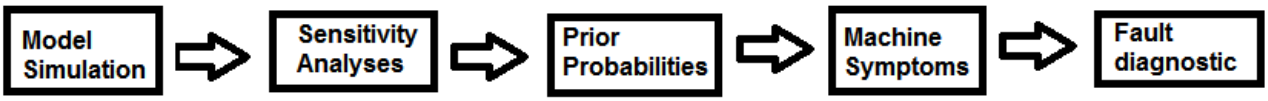

Figure 1 - Flowchart of experimental procedures.

2.1 Bayesian Networks

Bayesian Networks are a probabilistic graphical model that represents the random variables as nodes, and the links between nodes as conditional probabilities (Bishop, 2006). The Figure 2 represents a simple Bayesian Network.

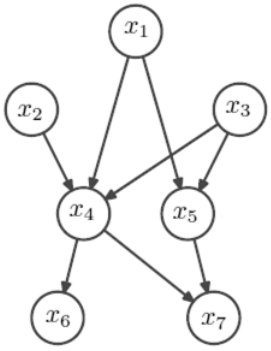

Figure 2 - Simple Bayesian Network (Bishop, 2006)

The nodes without any input arrows (x_1, x_2, x_3) are called root nodes, and the nodes that received the arrows are called child nodes. The joint probability distribution is represented by the Equation 1 (Bishop, 2006):

$$p(x) = \prod_{k=1}^{k} p(x_k|pa_k) \quad (1)$$

Where pa_k denotes the set of parents of x_k, and $x = \{x_1, x_2, x_3 \ldots x_k\}$. Once that the $p(x_k|pa_k)$ is the conditional probability between nodes and their parents, the probability of the root nodes are the prior probability.

The advantage of Bayesian Networks relays on the independence assumption. For instance, if a conditional probability table was construct for this network, it will need 2^k inputs, where k s the number of nodes. In this context, on Bayesian Networks the probability of a node depends only of the parents' nodes, so the number of inputs for calculated the probability of a node will decrease, and this calculation will be feasible. On this work, all variables are assumed as Boolean, so each variable can assume two states, true or false. In this context, the prior probabilities of the roots nodes, and the conditional probabilities of the other nodes on network were represented by two states. Table 1 shows all the probabilities of roots nodes and Table 2 shows all the conditional probabilities assumed to represented the states of each node.

Table 1 - Probabilities for roots nodes.

Roots Nodes	**State = True**	**State = False**
(a) Periodical Fatigue	p(a) = 0.15	p(â) = 0.85
(b) Medium Corrosive	p(b) = 0.2	p(b) = 0.8
(c) Overload	p(c) = 0.2	p(c) = 0.8

(d) Improper start/stop	p(d) = 0.1	p(d) = 0.9
(e) Begrime	p(e) = 0.2	p(e) = 0.8
(f) Rupture	p(f) = 0.1	p(f) = 0.9
(g) Initial bending	p(g) = 0.2	p(g) = 0.8

Table 2 - Conditional Probability of child nodes.

Conditional Probability of child nodes			
$p(A|a,b) = 0.65$	$p(C|e,f,g) = 0.9$	$p(x|A,C) = 0.9$	$p(y|A,B,C) = 0.9$
$p(A|\bar{a},b) = 0.5$	$p(C|\bar{e},f,g) = 0.9$	$p(x|\bar{A},C) = 0.8$	$p(y|\bar{A},B,C) = 0.8$
$p(A|a,\bar{b}) = 0.5$	$p(C|e,\bar{f},g) = 0.9$	$p(x|A,\bar{C}) = 0.5$	$p(y|A,\bar{B},C) = 0.8$
$p(A|\bar{a},\bar{b}) = 0.01$	$p(C|e,f,\bar{g}) = 0.9$	$p(x|\bar{A},\bar{C}) = 0.2$	$p(y|A,B,\bar{C}) = 0.8$
$p(B|c,d) = 0.9$	$p(C|\bar{e},\bar{f},g) = 0.8$	$p(z|A,C) = 0.9$	$p(y|\bar{A},B,\bar{C}) = 0.8$
$p(B|\bar{c},d) = 0.7$	$p(C|\bar{e},f,\bar{g}) = 0.9$	$p(z|\bar{A},C) = 0.2$	$p(y|\bar{A},\bar{B},C) = 0.6$
$p(B|c,\bar{d}) = 0.8$	$p(C|e,\bar{f},\bar{g}) = 0.8$	$p(z|A,\bar{C}) = 0.8$	$p(y|A,\bar{B},\bar{C}) = 0.7$
$p(B|\bar{c},\bar{d}) = 0.1$	$p(C|\bar{e},\bar{f},\bar{g}) = 0.1$	$p(z|\bar{A},\bar{C}) = 0.1$	$p(y|\bar{A},\bar{B},\bar{C}) = 0.1$

2.2 Mathematical Model

The finite element method was used to modelling the rotor system, as described by Nelson (1980), where 18 nodes (Figure 3) represented the rotor. The rotor is composed of a steel shaft with x mm length and w mm diameter (E = $2.1 \cdot 10^{11}$Pa, ρ = 7860 kg/m^3, G = $0.796 \cdot 10^{11}$); two rigid discs D1 (node 5 with 2,3084 kg), and D2 (node 14 with 2,3084 kg), with 12 mm intern diameter and 90 mm external diameter; and four bearings (located at nodes 3, 7, 12 and 16 respectively). A flexible coupling is located between nodes 9 and 10. This coupling is modeled by the second model of Nelson Crandall (Tadeo and Cavalca, 2003). The mass in each coupling node is 0.0556. The stiffness and damping coefficients are…. The equation of motion is represented by the matrix of mass **M**, stiffness **K**, damping **C**, which takes into account the stiffness matrix **K** multiplied by the constant β and the gyroscopic matrix multiplied by the rotating speed ω (**C** = $\beta \cdot$**K** + $\omega \cdot$**G**), the vector containing the excitation force **f**(t) and the vector of nodal displacement **δ**, which is composed by the rotor-bearing system degrees of freedom $\boldsymbol{\delta}(t)^t = \{y_1, z_1, \phi_{y_1}, \phi_{z_1}, \dots, y_n, z_n, \phi_{y_n}, \phi_{z_n}\}$ (Equation 2). This paper considers three excitation forces, the unbalanced force, the misalignment force and the force generated by the cracks.

$$\mathbf{M}\ddot{\boldsymbol{\delta}}(t) + \mathbf{C}\dot{\boldsymbol{\delta}}(t) + \mathbf{K}\boldsymbol{\delta}(t) = \mathbf{f}(t) \tag{2}$$

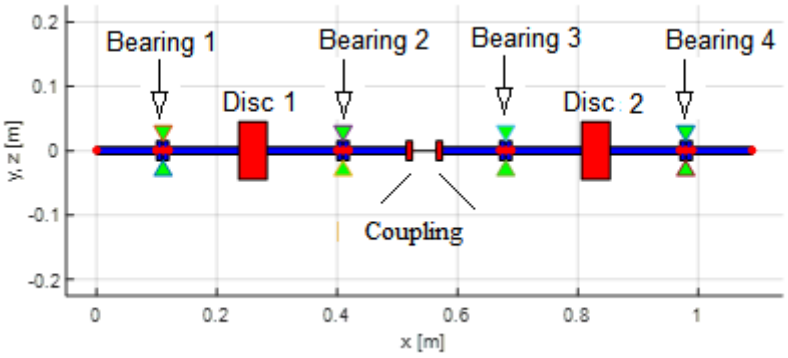

Figure 3 - Finite Element Model of rotor system.

The global system matrices must contain the characteristics of the bearings at the connection points with the shaft, so the bearing stiffness $\mathbf{K_m}$ and damping $\mathbf{C_m}$ matrices should be added to the global stiffness and damping matrices in the degrees of freedom related to the bearings. These matrices take into account the direct and cross stiffness and damping coefficients. The bearing stiffness and damping matrices are written as follows:

$$\mathbf{K_m} = \begin{bmatrix} & \vdots & \vdots & \\ \dots & K_{yy} & K_{yz} & \dots \\ \dots & K_{zy} & K_{zz} & \dots \\ & \vdots & \vdots & \end{bmatrix} \qquad \mathbf{C_m} = \begin{bmatrix} & \vdots & \vdots & \\ \dots & C_{yy} & C_{yz} & \dots \\ \dots & C_{zy} & C_{zz} & \dots \\ & \vdots & \vdots & \end{bmatrix} \tag{3}$$

2.2 Unbalanced Force

The unbalanced force is modeled as the product of unbalanced mass and the distance between the unbalanced mass and the geometric center of the rotary axis. The amplitude varies with the rotation speed squared. The Figure 4 shows the unbalanced mass, represented by m_{UNB}, e is the eccentricity, φ is the phase angle of the unbalance, ω is the shaft rotating speed and f_{UNB} is the unbalanced force, being f^z_{UNB} and f^y_{UNB} the horizontal and vertical components, respectively.

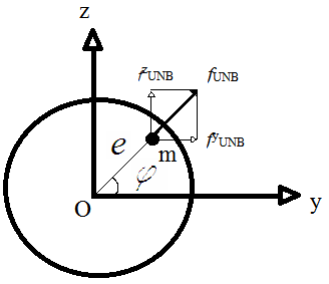

Figure 4 - Unbalanced mass scheme.

The Equation 3 represents the unbalance force, where m is the unbalanced mass, e is the eccentricity, ω is the rotating speed and φ is the phase angle.

$$\mathbf{f_{unb}}(t) = m \cdot e \cdot \omega^2 \begin{Bmatrix} \vdots \\ \cos(\omega t - \varphi) \\ \sin(\omega t - \varphi) \\ \vdots \end{Bmatrix} \tag{3}$$

The unbalance response is showed on Fig. 5, where the first and second critical speed were on approximal at 74 and 86 Hz respectively.

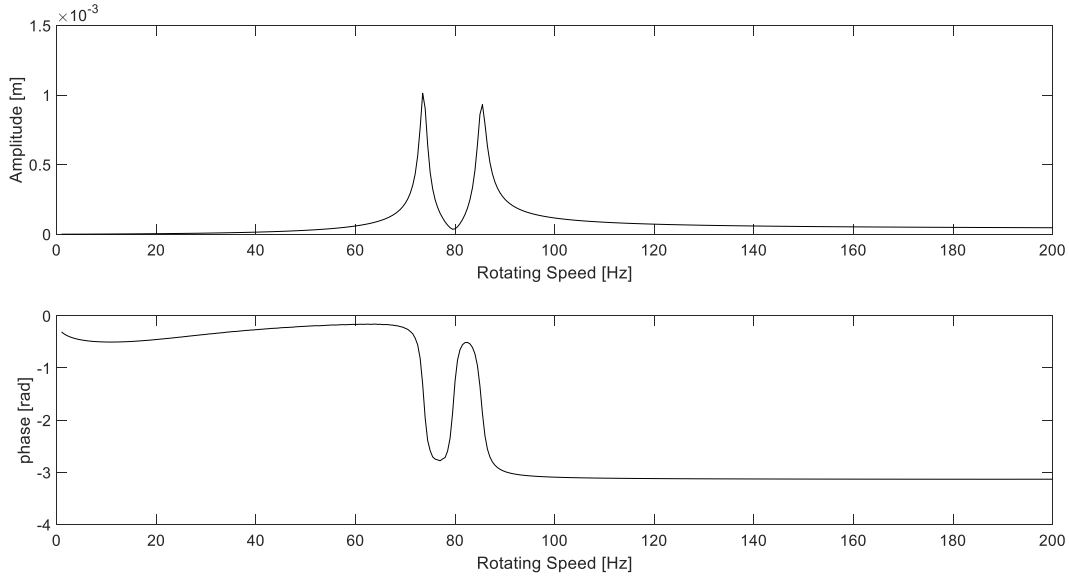

Figure 5 – Unbalance Response.

2.3 Shaft Misalignment

The model adopted for represent the forces and moments of misalignment is the Gibbons (1976). This model considers the moments and forces constants at the couplings. The misalignment considered on this works is the parallel misalignment, and for that, two nodes on the finite element model represented the misalignment, as Figure 6 shows.

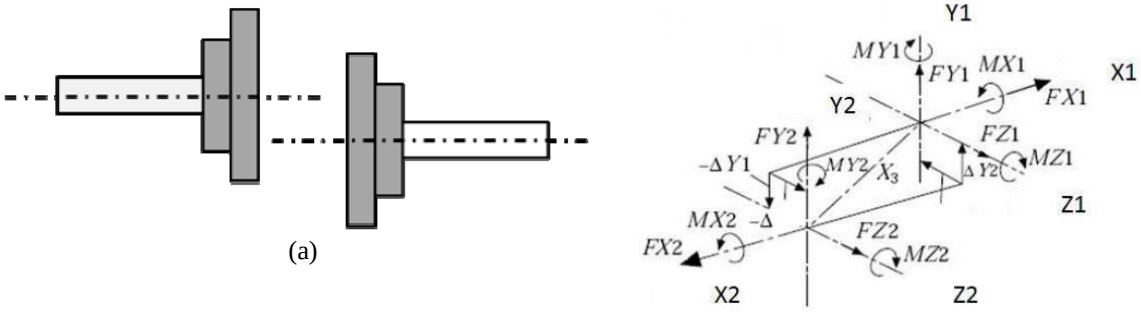

(a) (b)

Figure 6 - (a) Parallel Misalignment, (b) Misalignments moments and forces

The centerline of the drive shaft and the driven shaft are the X2 and X1, while the forces and moments generated by misalignment are represented as F_{X1}, F_{X2}, F_{Y1}, F_{Y2}, F_{Z1}, F_{Z2}, M_{X1}, M_{X2}, M_{Y1}, M_{Y2}, M_{Z1} and M_{Z2}. The Equation 4 shows the misalignment angles, the Eq. 5 the misalignment's moments, and the Eq. 6 the misalignment's forces.

$$\theta_1 = \sin^{-1}\left({}^{\Delta y_1}/_{X_3}\right) \qquad \emptyset_1 = \sin^{-1}\left({}^{\Delta z_1}/_{X_3}\right)$$
$$\theta_2 = \sin^{-1}\left({}^{\Delta y_2}/_{X_3}\right) \qquad \emptyset_2 = \sin^{-1}\left({}^{\Delta z_2}/_{X_3}\right) \tag{4}$$

$$M_{y1} = T_Q \cdot \sin(\theta_1) + K_b \cdot \emptyset_1 \qquad M_{Z1} = T_Q \cdot \sin(\emptyset_1) - K_b \cdot \theta_1 \qquad M_{X1} = T_Q$$
$$M_{y2} = T_Q \cdot \sin(\theta_2) + K_b \cdot \emptyset_2 \qquad M_{Z2} = T_Q \cdot \sin(\emptyset_2) - K_b \cdot \theta_2 \qquad M_{X2} = -T_Q \tag{5}$$

$$F_{y1} = \frac{(-M_{y1} - M_{y2})}{X_3} \qquad F_{y2} = -F_{y1}$$
$$F_{z1} = \frac{(M_{y1} + M_{y2})}{X_3} \qquad F_{z2} = -F_{z1} \tag{6}$$
$$F_{x1} = K_a \cdot \Delta x + K_A(\Delta x)^3 \qquad F_{x2} = F_{x1}$$

The T_Q is the transmitted torque, K_a and K_A are the axial stiffness of the coupling (linear and nonlinear respectively), K_b is the diaphragm by coupling bending stiffness and Δx is the elongation (+) or compression (-) of the coupling with respect to its free length.

2.4 Crack

The modelling of a cracked rotor following the work of Al-Shudeifat (2013). On that paper, the author uses the finite element method to model the cracked rotor. For that, he considers the behaves of a cracked rotor as an asymmetric shafts, and the moments of inertia of the cracked section was taken into account on the formulation of the finite element modelling of the stiffness matrix. As defined at work of Al-Shudeifat (2013), the centroid area moments of inertia with relation to the axis $\bar{X}$ and $\bar{Y}$ are constants and with relation to axis $\bar{x}$ and $\bar{y}$ are varying with time. Figure 7 shows the cross section of the cracked element before and after the rotation.

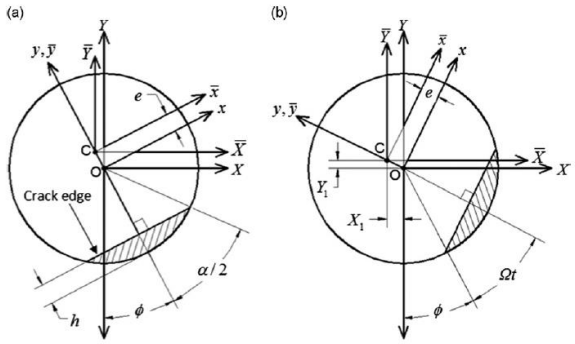

Figure 7 - Shaft with element cracked: (a) cracked element before rotation, (b) cracked element after rotation (Al-Shudeifat, 2013).

Equation 7 define the centroid area moments of inertia of the cracked element with relation to the fixed axis $\bar{X}$ and $\bar{Y}$, as is defined at Al-Shudeifat (2013).

$$I_{\bar{x}}(t) = \frac{I_{\bar{x}} + I_{\bar{y}}}{2} + \frac{I_{\bar{x}} - I_{\bar{y}}}{2} cos(2\Omega t) + I_{\bar{x}\bar{y}} sin(2\Omega t)$$

$$I_{\bar{Y}}(t) = \frac{I_{\bar{x}} + I_{\bar{y}}}{2} - \frac{I_{\bar{x}} - I_{\bar{y}}}{2} cos(2\Omega t) - I_{\bar{x}\bar{y}} sin(2\Omega t) \tag{7}$$

$$I_{\bar{X}\bar{Y}}(t) = -\frac{I_{\bar{x}} - I_{\bar{y}}}{2} sin(2\Omega t) + I_{\bar{x}\bar{y}} cos(2\Omega t)$$

The centroid area moments of inertia with respect to the rotating axis $\bar{x}$ and $\bar{y}$ are defined by Eq. 8, with $0 \leq \mu \leq 1$ (Al-Shudeifat, 2013).

$$I_x = \frac{\pi R^4}{4} + \frac{R^4}{4}\left((1-\mu)(2\mu^2 - 4\mu + 1)\Upsilon + \sin^{-1}(1-\mu)\right)$$

$$I_y = \frac{\pi R^4}{4} - \frac{R^4}{12}\left((1-\mu)(2\mu^2 - 4\mu - 3)\Upsilon + 3\sin^{-1}(\Upsilon)\right) \tag{8}$$

Where $\Upsilon = \sqrt{\mu(2-\mu)}$ and $\mu = {}^{h}/_{R}$ is the non-dimensional crack deph.

Once that the moments of inertia were calculated, the stiffness matrix will change, so the new equation of motion (Equation 9) can be written as (Al-Shudeifat, 2013).

$$\mathbf{M\ddot{\delta}}(t) + \mathbf{C\dot{\delta}}(t) + \left(\mathbf{K_1} + \mathbf{K_2 cos}(2\Omega t) + \mathbf{K_3 sin}(2\Omega t)\right)\boldsymbol{\delta}(t) = \mathbf{F_{unb}}(t) + \mathbf{F_{mis}}(t) + \mathbf{F_g} \tag{9}$$

The solution of the system is expressed as a finite Fourier series (Equation 10).

$$\delta(t) = \boldsymbol{A_0} + \sum_{k=1}^{n} (\boldsymbol{A_k} cos(k\Omega t) + \boldsymbol{B_k} sin(k\Omega t)) \tag{10}$$

$$\begin{bmatrix} K_1 & 0 & 0 & 0.5K_2 & 0.5K_3 & 0 & 0 & 0 & 0 & \cdots & 0 & 0 \\ 0 & C^{(1)} + C_2 & C_1^{(1)} + C_2 & 0 & 0 & C_2 & C_3 & 0 & 0 & \cdots & 0 & 0 \\ 0 & -C_1^{(1)} + C_2 C^{(1)} - C_2 & & 0 & 0 & -C_3 & C_2 & 0 & 0 & \cdots & 0 & 0 \\ K_2 & 0 & 0 & C^{(2)} & C_1^{(2)} & 0 & 0 & C_2 & C_3 & \ddots & 0 & 0 \\ K_3 & 0 & 0 & -C_1^{(2)} & C^{(2)} & 0 & 0 & -C_3 & C_2 & \ddots & \vdots & \vdots \\ 0 & C_2 & C_3 & 0 & 0 & C^{(3)} & C_1^{(3)} & 0 & 0 & \ddots & 0 & 0 \\ 0 & -C_3 & C_2 & 0 & 0 & -C_1^{(3)} & C^{(3)} & 0 & 0 & \ddots & C_2 & C_3 \\ 0 & 0 & 0 & C_2 & C_3 & 0 & 0 & C^{(4)} & C_1^{(4)} & \ddots & -C_3 & C_2 \\ 0 & 0 & 0 & -C_3 & C_2 & 0 & 0 & -C_1^{(4)} & C^{(4)} & \ddots & 0 & 0 \\ \vdots & \vdots & \vdots & \ddots & \ddots & \ddots & \ddots & \ddots & \ddots & 0 & C^{(n)} & C_1^{(n)} \\ 0 & 0 & 0 & 0 & \cdots & 0 & C_2 & C_3 & 0 & 0 & -C_1^{(n)} & C^{(n)} \end{bmatrix} \begin{bmatrix} A_0 \\ A_1 \\ B_1 \\ A_2 \\ B_2 \\ A_3 \\ B_3 \\ A_4 \\ B_4 \\ \vdots \\ A_n \\ B_n \end{bmatrix} = \begin{bmatrix} F_g \\ F_{unb_1} \\ F_{unb_2} \\ F_{mis1} \\ F_{mis2} \\ 0 \\ 0 \\ 0 \\ 0 \\ \vdots \\ 0 \\ 0 \end{bmatrix} \tag{11}$$

Where $C_2 = \frac{1}{2} K_2; C_3 = \frac{1}{2} K_3; C^{(j)} = K_1 - (j\Omega)^2 M$ and $C_1^{(j)} = j\Omega C$ for j = 1,2,…,n and n is the number of harmonics used.

3. SENSITIVITY ANALYSES

In order to analyze the effects of included the unbalance, parallel misalignment and crack faults on simulation model, the rotor vibration amplitude was analyzed in 5 rotational speeds, for the two critical rotor speeds (74 and 86 Hz). The velocities chosen were ⅓ of the critical speed (25 and 28 Hz), ½ of the critical speed (38 and 43 Hz), just below the critical speed (70 and 80 Hz), at critical speed (74 and 86 Hz) and just above them (90 Hz). The values of the vibration amplitude was taken on the 1X, 2X and 3X vibration, for each rotation.

For the sensitivity analysis, a factorial design (Montgomery, 2001) was used, which consists of combining all the effects introduced in the experiment and quantifying the effect on the system response. For this, two values for each fault was chosen, so the factorial design was defined with 2 levels and 3 variables, thus totaling 8 combinations. Table 3 shows the chosen values for each variable, and the way that these values were put on the table, the variables of A was taken first the smaller value than the bigger, the variable B is two smaller values than two bigger values and the variable C is four smaller values than the four bigger values.

Table 3 - Values used for sensitivity analyses

ω	Exp	Crack	Misalignment				Unb	A	B	C
		μ	Δx_1	Δx_2	Δy_1	Δy_2	m·e			
ω	1	0.6	$2 \cdot 10^{-3}$	$-2 \cdot 10^{-3}$	$-2 \cdot 10^{-3}$	$2 \cdot 10^{-3}$	$1 \cdot 10^{-4}$	-1	-1	-1
	2	0.8	$2 \cdot 10^{-3}$	$-2 \cdot 10^{-3}$	$-2 \cdot 10^{-3}$	$2 \cdot 10^{-3}$	$1 \cdot 10^{-4}$	+1	-1	-1
	3	0.6	$4 \cdot 10^{-3}$	$-4 \cdot 10^{-3}$	$-4 \cdot 10^{-3}$	$4 \cdot 10^{-3}$	$1 \cdot 10^{-4}$	-1	+1	-1
	4	0.8	$4 \cdot 10^{-3}$	$-4 \cdot 10^{-3}$	$-4 \cdot 10^{-3}$	$4 \cdot 10^{-3}$	$1 \cdot 10^{-4}$	+1	+1	-1
	5	0.6	$2 \cdot 10^{-3}$	$-2 \cdot 10^{-3}$	$-2 \cdot 10^{-3}$	$2 \cdot 10^{-3}$	$3 \cdot 10^{-4}$	-1	-1	+1
	6	0.8	$2 \cdot 10^{-3}$	$-2 \cdot 10^{-3}$	$-2 \cdot 10^{-3}$	$2 \cdot 10^{-3}$	$3 \cdot 10^{-4}$	+1	-1	+1
	7	0.6	$4 \cdot 10^{-3}$	$-4 \cdot 10^{-3}$	$-4 \cdot 10^{-3}$	$4 \cdot 10^{-3}$	$3 \cdot 10^{-4}$	-1	+1	+1
	8	0.8	$4 \cdot 10^{-3}$	$-4 \cdot 10^{-3}$	$-4 \cdot 10^{-3}$	$4 \cdot 10^{-3}$	$3 \cdot 10^{-4}$	+1	+1	+1

In order to make the combinations, the variables of unbalance moment, misalignment and crack was put into a cube, and the vertices of this cube represents the vibration amplitude response for each combination of faults values. The variable A is the crack, B is the misalignment and C is the unbalanced moment. In this way, the main effects (A, B and C), the interactions of the factors (AB, AC and BC) and the three factors together (ABC) can be observed.

4. RESULTS

The topology of the Bayesian Network was done with previous knowledge, like the probable causes for the rotor presents crack, misalignment and unbalance. These causes are linked to the faults and the faults are linked to the symptoms, like Figure 8 shows.

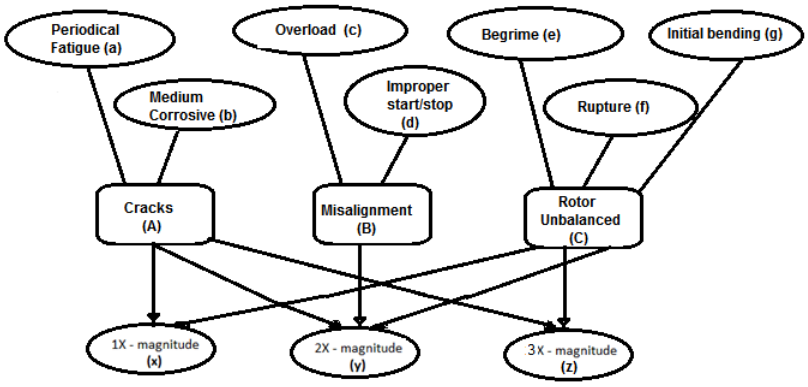

Figure 8 - Topology of Bayesian Network

For simulate the Bayesian Network, it was adopted some initial probabilities and conditional probabilities for each node. These probabilities were adopted taking into account the results of factorial design. Figures 9 and 10 shows the main effects of each variable, and two and three factor interactions, for 1X, 2X and 3X in all the velocities analyzed. It´s possible to realized that for the critical velocities the effects were more significant than the others, besides that at ½ of the first critical velocity on 2X and on 3X the crack effects was bigger that the same effect at others velocity. This behavior was noticeable at ½ of the second critical velocity on 2X too. At critical velocity, the effects of crack and unbalanced moment was prevailing, on 1X and 3X. The effect of misalignment was too small, but it was notice that when this effect was combined with the other two effects, it has influence on 2X.

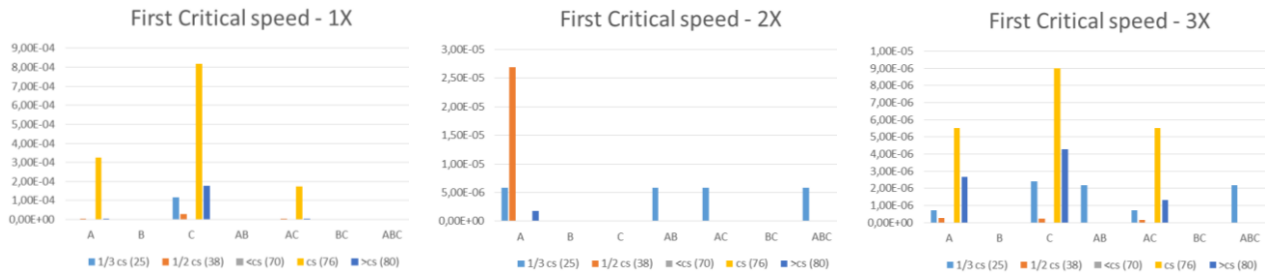

(a) (b) (c)

Figure 9 - Main effects and it´s interactions for all rotations analyzed (first critical speed): (a) 1X, (b) 2X and (c) 3X.

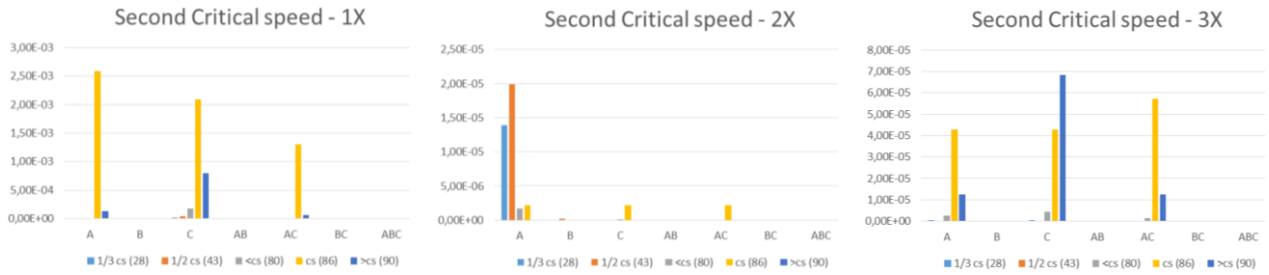

(a) (b) (c)

Figure 10 - Main effects and it´s interaction for all rotations analyzed (Second critical speed): (a) 1X, (b) 2X and (c) 3X.

In order to showing the results with more clearly, the mean of each effect was calculated for 1X, 2X and 3X (Figure 11). For 1X, the predominant effect was the unbalanced moment, follow by the crack effect, and both effects combined. On the other hand, at 2X the crack has a lot of influence, and the misalignment appears when combined with crack and when three effects are together. For the 3X harmonic, the unbalanced moment and the crack has influence, although the influence of unbalanced moment has more influence because of the crack. To conclude this, another simulation was done with just one failure, and when only the unbalanced moment was considered, the only harmonics that he has influence was on the 1X.

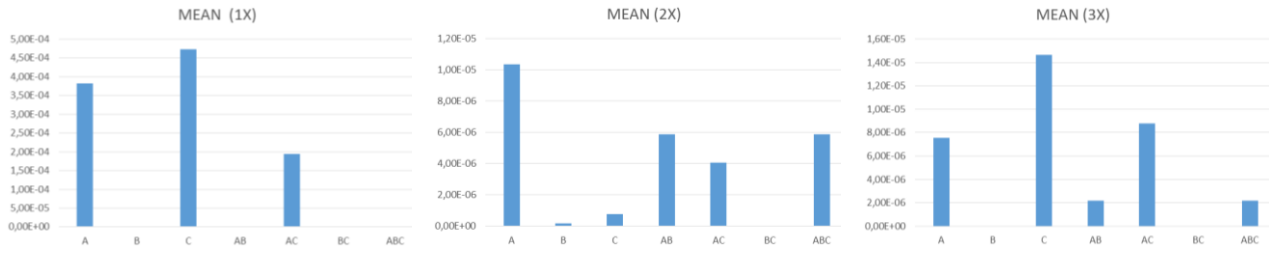

(a) (b) (c)

Figure 11 - Mean of main effects and it´s interaction, (a) 1X, (b) 2X and (c) 3X.

Using these values, the Bayesian Network calculates the probability of the faults, given the symptoms. The Table 4 shows the results:

Table 4 - Probability of fault

Symptom	**Probability of Fault**		
(1X) and (2X)	P(A) = 5.12%	P(B) = 33.91%	P(C) = 86.91%
(1X) and (3X)	P(A) = 54.80%	P(B) = 19.58%	P(C) = 52.89%
(2X) and (3X)	P(A) = 57.25%	P(B) = 41.18%	P(C) = 33.24%
(1X), (2X) and (3X)	P(A) = 59.35%	P(B) = 32.17%	P(C) = 78.12%

Table 4 considers the symptoms as true or false. In this context, four cases were analyses, the first one is the case where the symptom 1X and 2X are true, so the most probable fault is the unbalance with 86.91%, and the misalignment with 33.91%, the probability of the crack is too low, 5.12%. This is because the symptom on 1X is influence almost all by the unbalance, and the misalignment have more influence on 2X. The second case is considering the symptoms 1X and 3X as true; in this case the most probable fault is the crack with 54.80%, and the unbalance with 52.89%. These values could be consistent because the symptom 3X are considered as true, and the crack has a lot influence on these symptom, while the unbalance has influence on 1X, as mentioned before.

When the case one is compared with case two, it´s possible conclude that the crack has influence also in 1X, because the probability of crack fault is bigger than the unbalance, and this failure in particularly has influence only in 1X, as the case one shows. The case three considered the symptom 1X and 2X as true, in this case the most probable fault is the crack, with 57.25%, and the misalignment with 41.18%. The unbalance appears with 33.24%, but this is because the unbalance always appears. On this case, it´s possible to conclude that the misalignment, in this model, has influence only on 2X, and the crack has influence on all the symptoms, especially on 3X.

The last case considers all symptom as true, 1X, 2X and 3X are true, so in this case, the most probable fault is the unbalance, with 78.12%, as mentioned before, always that the symptom 1X is considered the unbalance appears. The crack fault has 59.35% of probability, because it has influence on all symptoms, and the misalignment has 32.17% of probability, it is consistent because the symptom 2X is considered. The cases when it could be only one symptom wasn´t considered because it will be inconsistent, once that the rotating machine will always present a little unbalance or misalignment, despite the machine being balanced and aligned.

5. CONCLUSION

This works proposed the diagnose of faults in rotating machines using Bayesian Networks, considering the symptoms of the system. To do this, a few simulations was done and a sensitivity analyzes was applied on these results, in order to building the topology of the Bayesian Network. Once that the variables on the network was considered as Booleans variables, each variable has two states. The Bayesian Networks calculated the probability of fault, given the conditional probability of each symptom (amplitude at 1X, 2X and 3X). The results were consistent with the present literature, the unbalance moment has main influence on first harmonic, and the crack has influence on all the harmonics considered, especially on 3X. The misalignment shows a little influence on 2X, but it could be because on this model considerate the misalignment has small influence. On the other hand, the methodology adopted showed to be efficiently.

6. ACKNOWLEDGMENT

The authors thanks CAPES for providing financial support for this work. Acknowledgments are also extended to grant #2015/ 20363-6, São Paulo Research Foundation (FAPESP) and LAMAR/UNICAMP.

7. REFERENCES

Al-Shudeifat , M. A. 2013. On the finite element modeling of the asymmetric cracked rotor, Journal of Sound and Vibration, Volume 332, Issue 11, Pages 2795-2807, ISSN 0022-460X, https://doi.org/10.1016/j.jsv.2012.12.026.

Al Hussain, K.M.; Redmond, I., 2002. Dynamic response of two rotor connected by rigid mechanical coupling with parallel misalignment. Journal of Sound and Vibration, Volume 249, pages 483-498.

Bishop, 2006. Pattern Recognition and Machine Learn. Springer Science + Business Media, page 378.

Chen C.; Mo C., 2004. A method for intelligent fault diagnosis of rotating machinery. Digital Sign Processes, Volume 14, Issue 3, Pages 203-217.

Gibbons, 1976. Coupling Misalignment Forces, Proceedings of 5th Turbomachinery Symposium, Gas Turbine Laboratories, Texas A&M University, Pages 111-116.

Jun, H.; Kim, D., 2017. A Bayesian network-based approach for fault analysis. Expert Systems with Applications, Volume 81, 2017, Pages 332-348, ISSN 0957-4174, https://doi.org/10.1016/j.eswa.2017.03.056.

Lei Y. et al, 2008. A new approach to intelligent fault diagnosis of rotating machinery. Expert Systems with Applications, Volume 35, Issue 4, Pages 1593–1600.

Lal, M.; Tiwari, R., 2012. Multi-fault identification in simple rotor-bearing-coupling systems based on forced response measurements. Mechanism and Machine Theory, volume 51, pages 87-109.

Liu Z. et al, 2015. An approach for developing diagnostic Bayesian network based on operation procedures. Expert Systems with Applications, Volume 42, Issue 4, Pages 1917-1926, ISSN 0957-4174, https://doi.org/10.1016/j.eswa.2014.10.020.

Montegomery, D., 2001. Design and Analyses of Experiments. Fifth edition.

Nelson , H.D. 1980. A Finite Rotating Shaft Element Using Timoshenko Beam Theory, J. Mech. Des. 102,pages.793–803.

Sekhar, A.S.; Prabhu, B.S., 1995. Effect of coupling misalignment on vibration of rotating machines. Journal of Sound and Vibration, Volume 185, Pages 655-671.

Sahin F. et al, 2007. Fault diagnosis for airplane engines using Bayesian networks and distributed particle swarm optimization, Parallel Computing, Volume 33, Issue 2, 2007, Pages 124-143, ISSN 0167-8191, http://dx.doi.org/10.1016/j.parco.2006.11.005.

Tadeo, A. T., Cavalca, K. L. 2003. A Comparison of Flexible Coupling Models for Updating in Rotating Machinery Response. Journal of the Braz. Soc. of Mech. Sci. & Eng. Pages 235-246. http://dx.doi.org/10.1590/S1678-58782003000300004

Zhao Y.; Xiao F. and Wang S., 2012. An intelligent chiller fault detection and diagnosis methodology using Bayesian belief network. Energy and Buildings, Volume 57, 2013, Pages 278-288, ISSN 0378-7788, http://dx.doi.org/10.1016/j.enbuild.2012.11.007.

Xu, B. G., 2012. Intelligent fault inference for rotating flexible rotors using Bayesian belief network, In Expert Systems with Applications. Volume 39, Issue 1, Pages 816-822, ISSN 0957-4174, https://doi.org/10.1016/j.eswa.2011.07.079.

8. RESPONSIBILITY NOTICE

The authors are the only responsible for the printed material included in this paper.